HOKKAIDO UNIVERSITY

Title	Electrodeless photo-assisted electrochemical etching of GaN using a H3PO4-based solution containing S2O82- ions
Author(s)	Toguchi, Masachika; Miwa, Kazuki; Horikiri, Fumimasa et al.
Citation	Applied Physics Express, 12(6), 066504 https://doi.org/10.7567/1882-0786/ab21a1
Issue Date	2019-05-31
Doc URL	https://hdl.handle.net/2115/78270
Rights	© 2019 The Japan Society of Applied Physics
Rights(URL)	https://creativecommons.org/licenses/by-nc-nd/4.0/
Type	journal article
File Information	TSATO_APEX2019.pdf

Hokkaido University Collection of Scholarly and Academic Papers : HUSCAP

Electrodeless photo-assisted electrochemical etching of GaN using a H_3PO_4-based solution containing $S_2O_8^{2-}$ ions

Masachika Toguchi[1]*, Kazuki Miwa[1], Fumimasa Horikiri[2], Noboru Fukuhara[2], Yoshinobu Narita[2], Takehiro Yoshida[2], and Taketomo Sato[1]

[1]*Research Center for Integrated Quantum Electronics, Hokkaido University, Sapporo, Hokkaido 060–0813, Japan*

[2]*SCIOCS CO., Ltd., Hitachi, Ibaraki 319–1418, Japan*

E-mail: toguchi@rciqe.hokudai.ac.jp

Electrodeless PEC etching was successfully demonstrated using a H_3PO_4-based solution containing $S_2O_8^{2-}$ ions. The pH value of the solution changed under UVC illumination, clearly showing that $SO_4^{\cdot-}$ radicals were produced from $S_2O_8^{2-}$ ions by absorbing UVC light. The production rate of $SO_4^{\cdot-}$ radicals kept a constant value in the wide pH range of the solution, leading to etching rates and surface roughness comparable with those obtained in KOH-based solutions. The positive-type photoresist was applicable as the etching mask for the H_3PO_4-based solution. This finding will contribute to a simple wet etching process suitable for the manufacturing of GaN-based devices.

Gallium Nitride (GaN) and related nitride semiconductors have been intensively studied for application to various optical and electronic devices such as light-emitting diodes [1, 2], UV lasers [3, 4], and high-frequency, high-power electronic devices [5-7]. In terms of the device fabrication process, etching is one of the most important factors affecting the device performance, namely, stability, reliability, and in-plane uniformity of device operation. For GaN-based devices, plasma-assisted dry etching, such as an inductive-coupled-plasma reactive-ion etching (ICP-RIE), has been commonly used because the alternative, wet chemical etching, is fairly difficult due to very strong chemical-bonding between nitrogen and III-group atoms [8]. However, there is serious problem in using a high-energy reaction in this way in that etching damage (such as nitrogen-vacancy defects and disordered atomic-bond arrangements) is induced on the surface [9, 10], leading to degraded performance of the device [11, 12].

Photo-assisted electrochemical (PEC) etching has been attracting attention as an easily controllable wet process in which the etching is conducted by supplying electric power to induce the anodic oxidation and its dissolution in the electrolyte [13-19]. Compared with dry-etching, PEC etching uses very little energy due to the nature of chemical reactions. Various applications of PEC etching have been reported for nitride semiconductors, including the removal of a surface damage layer [20] and the formation of a deep trench structure [21], mesa-structure GaN p-n junction diodes [22], and recessed-gate structure on AlGaN/GaN high-electron mobility transistors (HEMTs) [23-25].

Recently, simple electrodeless PEC etching or photo-assisted chemical etching utilizing a $S_2O_8^{2-}$ ion-containing solution has been reported [26-35]. The $S_2O_8^{2-}$ ion absorbs the UVC light with a wavelength λ below 310 nm and produces two sulfate radicals ($2SO_4^{\cdot-}$) [36, 37]. Since the $SO_4^{\cdot-}$ radical, which is a strongly oxidizing agent, functions as a cathode electrode in the PEC system [30, 32], a wired connection with electrochemical equipment is no longer necessary. Furthermore, our group has reported that the complicated electrochemical parameters can be translated into simple engineering parameters by optimizing the

arrangement of the UV light source.

In this study, we aimed to further simplify the electrodeless PEC etching process for the fabrication of GaN-based devices. In all previous reports (including our own), the etching has been conducted using a potassium hydroxide (KOH)-based solution. Therefore, a two-step patterning process was necessary for the fabrication of the etching mask, which was made of Ti or SiO_2 films, since the positive-type photoresist film could not be directly used as an etching mask due to its poor tolerance to alkaline solution. In this study, we utilize a phosphoric acid (H_3PO_4)-based solution with a weak acidity for the electrodeless PEC etching system. The basic properties of the pH change under UVC illumination were evaluated for a H_3PO_4-based solution containing $S_2O_8^{2-}$ ions through comparison with a KOH-based solution. Then, we successfully demonstrated the electrodeless PEC etching on an n-type GaN surface patterned with a positive-type photoresist mask.

The schematics of the experimental setup and sample used for the electrodeless PEC etching under UVC illumination are shown in **Fig. 1(a)** and **(b)**, respectively. Etching was conducted by dipping the sample into a 1:1 mixture containing 0.01 mol/L H_3PO_4 and 0.05 mol/L $K_2S_2O_8$ aqueous solution under illumination of UVC light. In some experiments, a KOH-based solution, namely, a 1:1 mixture containing 0.01 mol/L KOH and 0.05 mol/L $K_2S_2O_8$ aqueous solution, was used for comparison. In this study, the solutions were not stirred during the etching. As a light source, we used an SK-BUVC-0860 (Shikoh Tech LLC), which is a deep-UV flexible surface light with a luminous array film having a center wavelength λ of 260 nm and a full width at half maximum (FWHM) of 55 nm. The working distance from the light source to the sample surface was 40 mm, where the light power density of 4 mW/cm^2 was obtained in the atmosphere. The total amount of photons reaching the GaN surface strongly depended on the distance from the liquid surface, since the UVC light was absorbed in a solution containing $K_2S_2O_8$. In this study, the optical-path length in a solution was set to 5 mm, which is the same value as our previous study [35].

We used n-type GaN epitaxial layers grown by metal organic vapor phase epitaxy (MOVPE) on free-standing GaN (0001) substrates produced by a void-assisted separation (VAS) method [38, 39]. The carrier concentration, thickness, and threading dislocation density (TDD) of the n-type GaN layers were 5×10^{16} cm^{-3}, 3 μm, and 3×10^6 cm^{-2}, respectively. The sample size was 7×7 mm^2, which is much smaller than the illumination area of 80×60 mm^2. In this study, a positive-type photoresist film was utilized as an etching mask formed on the n-GaN surface, as shown in **Fig. 1(b)**. A Megaposit^{TM} SPR6810 was spin-coated at 500 rpm for 3 sec and 5000 rpm for 30 sec to obtain a 950-nm-thick film on the n-GaN surface. After a photo-lithography process, the patterned sample was hard-baked in an oven at 110°C for 10 min.

The pH value of the solution was measured using a multi pH-meter, PC700 (Eutech Instruments). Etching depth and morphology were evaluated using a surface profiler with a DEKTAK-150 (Bruker) and an atomic force microscope (AFM) with an L-trace II (Hitachi High-Tech Science Corporation).

The $S_2O_8^{2-}$ ion absorbs the UV light with $\lambda < 310$ nm and produces two $2SO_4^{\cdot -}$ radicals [36, 37]. The $SO_4^{\cdot -}$ radical is known as a strong oxidizing agent having a larger redox potential in a negative direction than that of hydrogen peroxide (H_2O_2) [40]. The $SO_4^{\cdot -}$ radical oxidizes the substance around itself and changes to the reduced form, sulfate ion (SO_4^{2-}), as $SO_4^{\cdot -} + e^- \rightarrow SO_4^{2-}$. Here, the photo-assisted chemical reaction of GaN in the present redox system is represented as

$$\mathrm{GaN} + \text{photo carriers}\ (3h^+ + 3e^-) + 3{SO_4}^{\cdot -} \rightarrow \mathrm{Ga^{3+}} + 3{SO_4}^{2-} + \frac{1}{2}\mathrm{N_2}, \qquad (1)$$

where the description of intermediate products (such as Ga_2O_3) is omitted for simplification.

As described in reaction (1), the photo-generated holes are used for the oxidation of the GaN surface, whereas the photo-generated electrons are consumed by the $SO_4^{\cdot-}$ radical. The $SO_4^{\cdot-}$ radical functions as a cathode in this reaction; that is, the outer cathode electrode is not necessary to perform the etching of GaN. Therefore, in this system, the production rate of $SO_4^{\cdot-}$ radicals from $S_2O_8^{2-}$ ions under UVC illumination is a key parameter to determine the etching rate of GaN.

Alternatively, the following reaction will occur by consuming the $SO_4^{\cdot-}$ radical:

$$SO_4^{\cdot-} + \frac{1}{2}H_2O \rightarrow SO_4^{2-} + H^+ + \frac{1}{4}O_2. \qquad (2)$$

Reaction (2) is a dominant reaction in this study, since the liquid surface irradiated with the UVC light is much larger than the reaction area on the GaN surface. Therefore, the pH variation measured over time gives us the information on the production rate of $SO_4^{\cdot-}$ radicals under UVC illumination.

Figure 2 compares the pH values of two kinds of $K_2S_2O_8$ containing solutions, where all data were obtained for every five minutes the UVC light was irradiated to the liquid surface. In the case of the KOH-based solution, the initial pH value was 11.79 in an alkali region, which was the result of mixing the strong alkali, KOH, and the weak acid, $K_2S_2O_8$. As the illumination time increased, the pH value decreased and reached an acid region at 45 min. The final pH value after 120 min of illumination was 1.96. In contrast, the initial pH value of the H_3PO_4–based solution started in an acid region. As the illumination time increased, the pH value gradually decreased from 2.37 to 1.79 after 120 min. These changes of pH values were observed only under illumination of UVC light; they were not observed under illumination of UVA light with $\lambda = 360$ nm.

As described in reaction (2), the $SO_4^{\cdot-}$ radical reacts with a water molecule and produces a H^+ ion. Therefore, the pH change, observed in the KOH-based solution, can be explained by the neutralization reaction with H^+ ions produced by consuming the $SO_4^{\cdot-}$ radicals. The pH value before and after the neutralization point is described as a function of the production rate of the H^+ ion $x = d[H^+]/dt$ and the illumination time t by

$$\mathrm{pH} = -\log_{10}\left(\frac{1.0\times10^{14}}{[OH^-]_i - x\cdot t}\right) \qquad \text{for pH} \geq 7 \qquad (3a)$$

and

$$\mathrm{pH} = -\log_{10}(x\cdot(t - t_n)) \qquad \text{for pH} < 7, \qquad (3b)$$

where t_n is the time it takes for the reaction to reach the neutralization point with pH = 7.0.

In the case of the KOH-based solution, the initial concentration of OH^- ions, $[OH^-]_i$, was 6.17×10^{-3} mol/L, which was estimated from the pH value of 11.79 at $t = 0$ min. The t_n of 40 min was obtained by drawing additional lines on the pH curve shown in **Fig. 2**. The result of curve fitting using Eqs. (3a) and (3b) is depicted as a dashed line in **Fig. 2**. The experimental data obtained for the KOH-based solution can be well reproduced by using the same fitting parameter x of 1.54×10^{-4} mol/Lmin, in both the alkali and acid regions. This result indicates that the $SO_4^{\cdot-}$ radicals were produced at a constant rate over a wide pH range, as the value of x corresponds to the production rate of the $SO_4^{\cdot-}$ radical under UVC illumination.

In the case of the H_3PO_4-based solution, the change of pH value can be considered the result of mixing acid solutions with each other. Thus, the pH change can be simply described by

$$\mathrm{pH} = -\log_{10}([H^+]_i + x\cdot t) \qquad \text{for pH} < 7, \qquad (4)$$

where the initial concentration of H^+ ions $[H^+]_i$ was 4.07×10^{-3} mol/L, obtained from the pH value of 2.39 at $t = 0$ min. The theoretical pH curve calculated using Eq. (4) is also shown in **Fig. 2** as a dashed line. Here, the same value of $x = 1.54 \times 10^{-4}$ mol/Lmin was used for the calculation. The slope of the experimental curve was slightly larger than that of the theoretical curve obtained using Eq. (4). This is probably because the pH change became

moderate due to the pH-buffering action in the H_3PO_4-based solution.

The electrodeless PEC etching was conducted on the GaN surface patterned with a photoresist film in the H_3PO_4-based solution under UVC illumination. **Figures 3(a)** and **(b)** shows the top image of the sample with the patterned-photoresist film before and after etching for 105 min, respectively. The line width of the lithography pattern was 10.6 μm, as shown in **(a)**. The pattern width was unchanged after the electrodeless PEC etching, indicating that the etching reaction occurred only in the open area following the lithography pattern. This result emphasizes the significant advantage of using the H_3PO_4-based solution, namely, that positive-type photoresist film can be utilized as an etching mask. **Figure 4** shows the correlation between the etching depth and the etching time. The red circle and blue square respectively indicate the present data and the previous data obtained on the SiO_2-masked GaN using the KOH-based solution [35]. We found that the etching depth increased linearly with time after some incubation period. The constant etching rate of 1.17 nm/min was obtained for the H_3PO_4-based solution, which is comparable with the etching rate of 1.0 nm/min obtained for the KOH-based solution. Their similar etching behavior can be consistently explained by the fact that the production rate of the $SO_4^{\cdot-}$ radicals was kept constant over the wide pH range.

The AFM images obtained on the sample after etching for 30 and 60 min are shown in **Fig. 5(a)** and **(b)**, respectively. Sharp corners were observed at the boundary between the etched and unetched surface after etching for 30 min, while the corners of the boundary were rounded after etching for 60 min. This is due to the poor adhesion of photoresist film on the GaN surface, which is expected to be improved by the optimization of a film-coating process. The roughness of the etched surface was 1.83 and 2.48 nm (root mean square: RMS), as determined from the AFM observation in the 7 × 7 μm^2 area. The surface morphology obtained here is also comparable to that obtained on the sample after etching in the KOH-based solution using a SiO_2-mask [35].

In conclusion, we succeeded in the electrodeless PEC etching of n-type GaN using a H_3PO_4-based solution containing $S_2O_8^{2-}$ ions. The pH value of the solution changed under UVC illumination, clearly showing that the $SO_4^{\cdot-}$ radicals were produced from $S_2O_8^{2-}$ ions by absorbing the UVC light. The production rate of the $SO_4^{\cdot-}$ radicals kept a constant value in the wide pH range of the solution. As a result, the etching rates and RMS roughness obtained in the H_3PO_4-based solution were about the same as those previously obtained in the KOH-based solutions. We also confirmed that the positive-type photoresist was suitable as the etching mask for the H_3PO_4-based solution. Our findings will contribute to n-GaN wet etching by enabling more simplicity and greater suitability for the photo-lithography process in the manufacturing of GaN-based devices.

Acknowledgments

This work was supported by JSPS KAKENHI - JP16H06421, JP17H03224.

References

1) J. I. Pankove, and J. E. Berkeyheiser, Proc. IEEE **60**, 1456 (1972).
2) S. Nakamura, T. Mukai, and M. Senoh, Appl. Phys. Lett. **64**, 1687 (1994).
3) S. Nakamura, M. Senoh, S. Nagahama, N. Iwasa, T. Yamada, T. Matsushita, H. Kiyoku, and Y. Sugimoto, Jpn. J. Appl. Phys. **35**, L74 (1996).
4) S. Nakamura, M. Senoh, S. Nagahama, N. Iwasa, T. Yamada, T. Matsushita, Y. Sugimoto, and H. Kiyoku, Appl. Phys. Lett. **69**, 4056 (1996).
5) B. J. Baliga, IEEE Electron Device Lett. **10**, 455 (1989).
6) U. K. Mishra, L. Shen, T. E. Kazior, and Y. F. Wu, Proc. IEEE **96**, 287 (2008).

7) T. Kachi, Jpn. J. Appl. Phys., **53**, 100210 (2014).
8) S. J. Pearton, J. C. Zolper, R. J. Shul, and F. Ren, J.Appl.Phys. **86**, 1 (1999).
9) X. A. Cao, H. Cho, S. J. Pearton, G. T. Dang, A. P. Zhang, F. Ren, R. J. Shur, L. Zhang, R. Hickman, and J. M. V. Hove, Appl. Phys. Lett. **75**, 232 (1999).
10) T. Hashizume, and R. Nakasaki, Appl. Phys. Lett. **80**, 4564 (2002).
11) Z. Mouffak, A. Bensaoula, and L. Trombetta, J. Appl. Phys. **2**, 727 (2004).
12) Z. Yatabe, J. T. Asubar, and T. Hashizume, J. Phys. D: Appl. Phys. **49**, 393001 (2016).
13) M. S. Minsky, M. White, and E. L. Hu, Appl. Phys. Lett. **68**, 1531 (1996).
14) C. Youtsey, I. Adesida, L. T. Romano, and G. Bulman, Appl. Phys. Lett. **72**, 560 (1998).
15) L. H. Peng, C. W. Chuang, J. K. Ho, C. N. Huang, and C. Y. Chen, Appl. Phys. Lett. **72**, 939 (1998).
16) I. M. Huygens, K. Strubbe, and E. P. Gomes, J. Electrochem. Soc. **147**, 1797 (2000).
17) T. Rotter, D. Mistele, J. Stemmer, F. Fedler, J. Aderhold, J. Graul, V. Schwegler, C. Kirchner, M. Kamp, and M. Heuken, Appl. Phys. Lett. **76**, 3923 (2000).
18) C. H. Ko, Y. K. Su, S. J. Chang, W. H. Lan, J. Webb, M. C. Tu, and Y. T. Cherng, Mater. Sci. Eng. B **96**, 43 (2002).
19) F. Horikiri, Y. Narita, and T. Yoshida, Jpn. J. Appl. Phys. **57**, 086502 (2018).
20) S. Matsumoto, M. Toguchi, K. Takeda, T. Narita, T. Kachi, and T. Sato, Jpn. J. Appl. Phys. **57**, 121001 (2018).
21) F. Horiki, H. Ohta, N. Asai, Y. Narita, T. Yoshida, and T. Mishima, Appl. Phys. Express **11**, 091001 (2018).
22) N. Asai, H. Ohta, F. Horikiri, Y. Narita, T. Yoshida, and T. Mishima, Jpn. J. Appl. Phys. **58,** SCCD05 (2019).
23) N. Harada, Y. Hori, N. Azumaishi, K. Ohi, and T. Hashizume, Appl. Phys. Express **4**, 021002 (2011).
24) Z. Zhang, S. Qin, K. Fu, G. Yu, W. Li, X. Zhang, S. Sun, L. Song, S. Li, R. Hao, Y. Fan, Q. Sun, G. Pan, Y. Cai, and B. Zhang, Appl. Phys. Express **9**, 084102 (2016).
25) Y. Kumazaki, K. Uemura, T. Sato, and T. Hashizume, J. Appl. Phys. **121**, 184501 (2017).
26) J. A. Bardwell, I. G. Foulds, J. B. Webb, H. Tang, J. Fraser, S. Moisa and S. J. Rolfe, J. Electron. Mater. **28**, L24 (1999).
27) H. Masher, D. W. DiSant, M. W. Dvorak, G. Soerensen, C. R. Bolognesi, J. A. Bardwell, H. Tang, and J. B. Webb, Electron. Lett. **36**, 1969 (2000).
28) H. Maher, D. W. DiSanto, G. Soerensen, and C. R. Bolognesi, Appl. Phys. Lett. **77**, 3833 (2000).
29) J. A. Bardwell, J. B. Webb, H. Tang, J. Fraser, and S. Moisa, J. Appl. Phys. **89**, 4142 (2001).
30) Z. H. Hwang, J. M. Hwang, H. L. Hwang, and W. H. Hung, Appl. Phys. Lett. **84**, 3759 (2004).
31) R. T. Green, W. S. Tan, P. A. Houston, T. Wang, and P. J. Parbrook, J. Electron. Mater. **36**, 397 (2007).
32) D. H. van Dorp, J. L. Weyher, M. R. Kooijman, and J. J. Kelly, J. Electrochem. Soc. **156**, D371 (2009).
33) J. L. Weyher, F. D. Tichelaar, D. H. van Dorp, J. J. Kelly, and A. Khachapuridze, J. Cryst. Growth **312**, 2607 (2010).
34) S. Lee, S. Mishkat-Ul-Masabih, J. T. Leonard, D. F. Feezell, D. A. Cohen, J. S. Speck, S. Nakamura, and S. P. DenBaars, Appl. Phys. Express **10**, 011001 (2017)
35) F. Horikiri, N. Fukuhara, H. Ohta, N. Asai, Y. Narita, T. Yoshida, T. Mishima, M. Toguchi, K. Miwa, and T. Sato, Appl. Phys. Express **12**, 031003 (2019).
36) R. P. Buck, S. Singhadeja, and L. B. Rogers, Anal. Chem. **26**, 1240 (1954).
37) L. Dogliotti, and E. Hayon, J. Phys. Chem. **71**, 2511 (1967).
38) Y. Oshima, T. Eri, M. Shibata, H. Sunakawa, K. Kobayashi, T. Ichihashi, and A. Usui,

Jpn. J. Appl. Phys. **42**, L1 (2003).
39) T. Yoshida, Y. Oshima, T. Eri, K. Ikeda, S. Yamamoto, K. Watanabe, M. Shibata, and T. Mishima, J. Cryst. Growth **310**, 5 (2008).
40) R.Memming, J. Electrochem. Soc. **116**, 785 (1969).

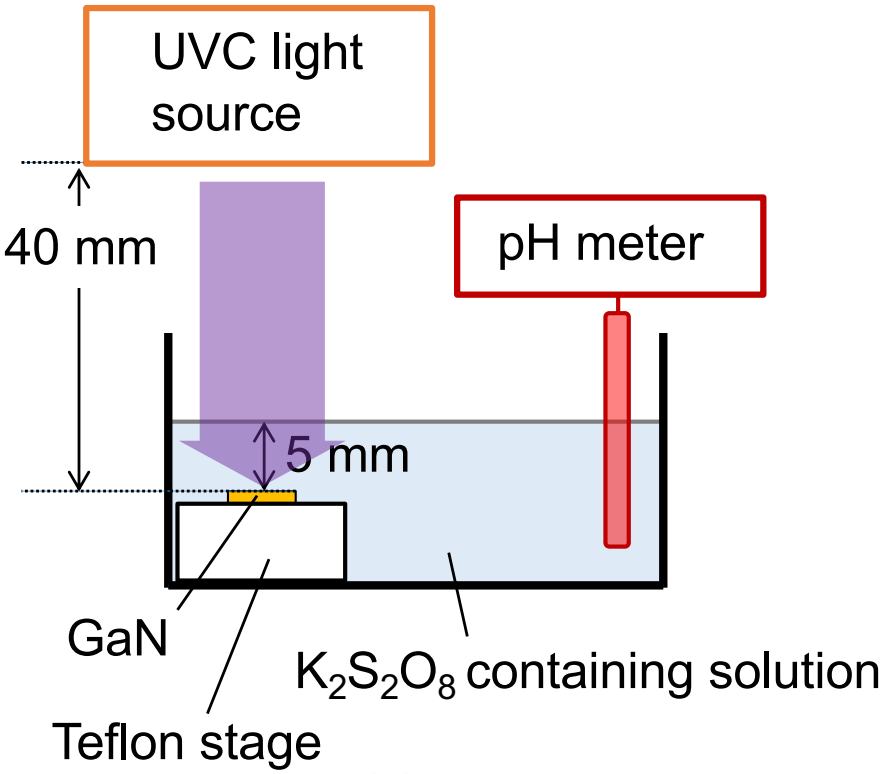

(a)

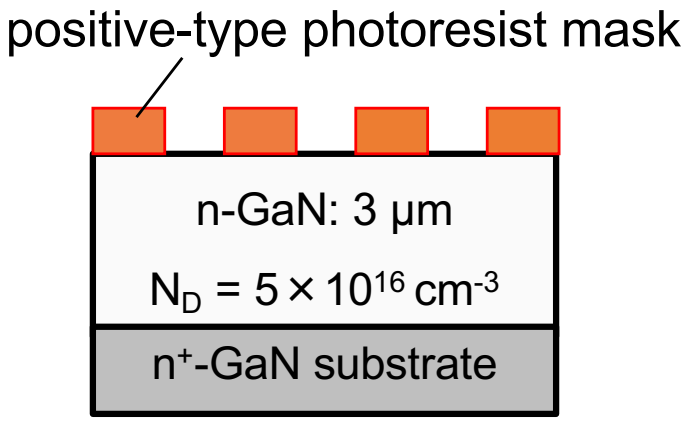

(b)

Fig. 1, Toguchi et al,

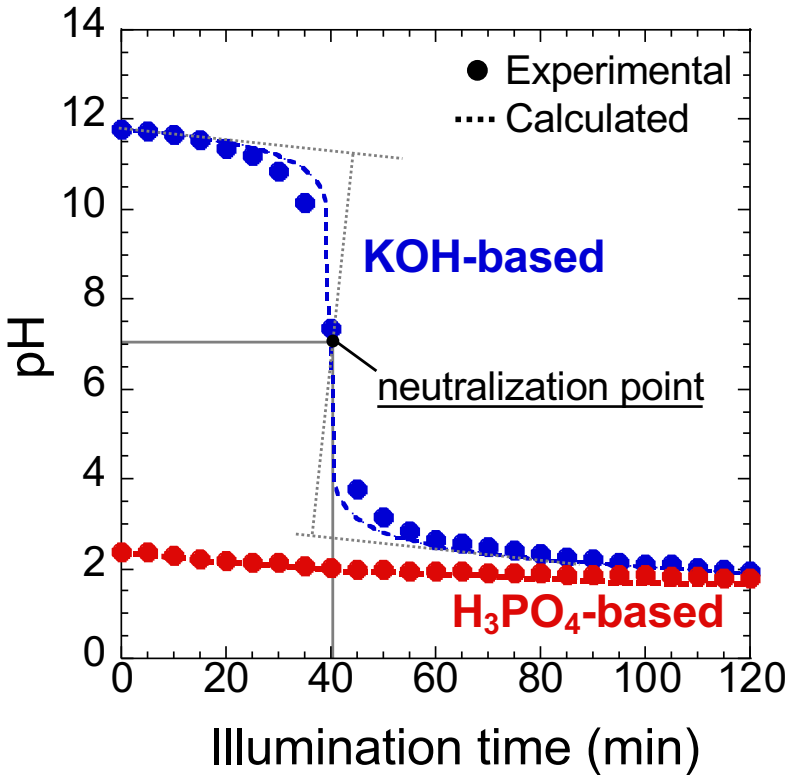

Fig. 2, Toguchi et al,

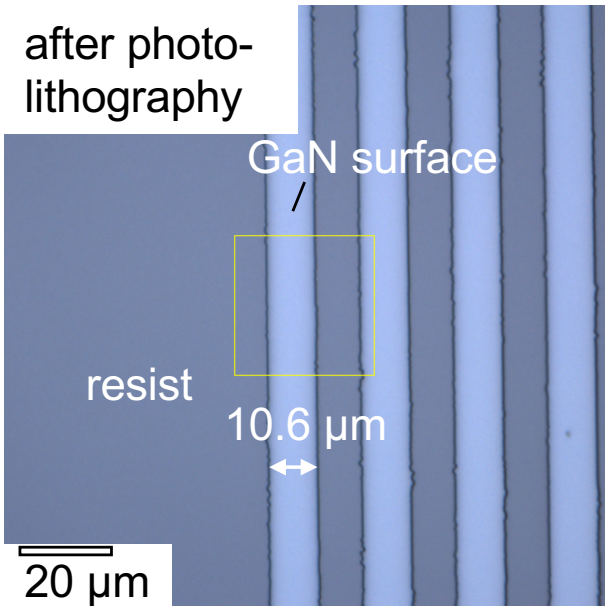

(a)

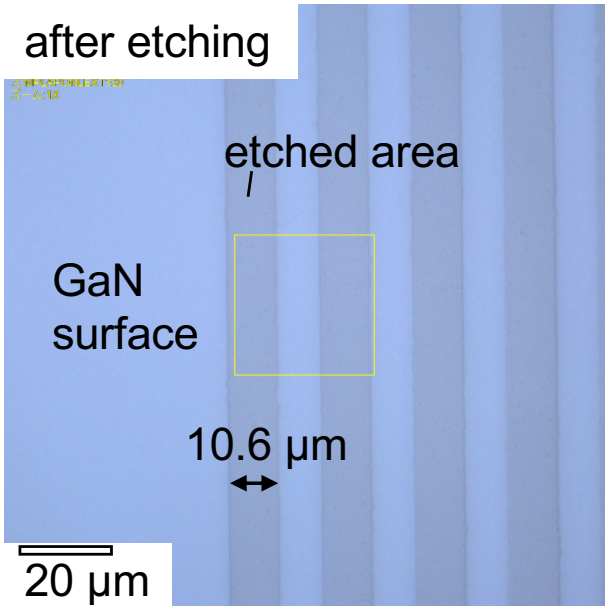

(b)

Fig. 3, Toguchi et al,

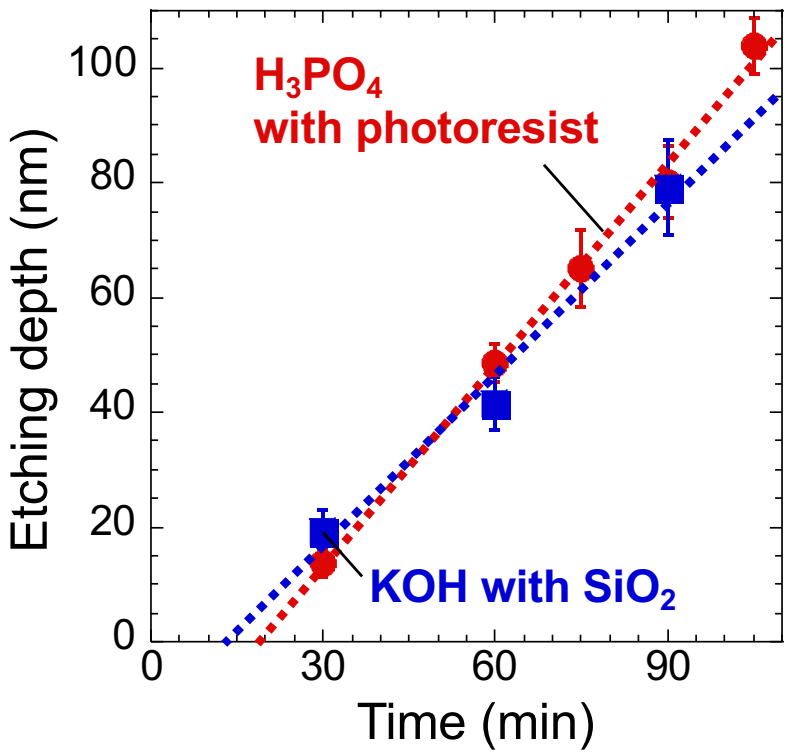

Fig. 4, Toguchi et al,

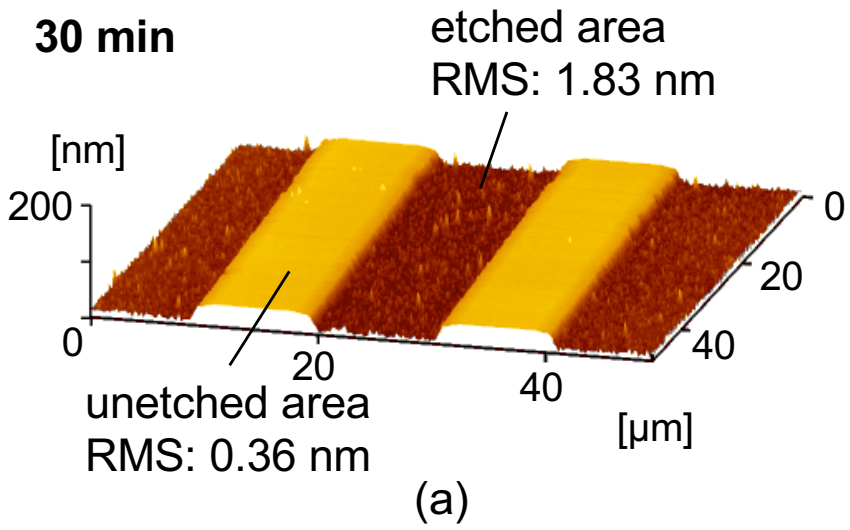

Fig. 5, Toguchi et al,